

## Conduction and trapping in electroluminescent polymer devices

Alasdair J. Campbell, Michael S. Weaver, David G. Lidzey, Donal D. C. Bradley, Ekkehard Werner, Wolfgang Brütting, Markus Schworer

### Angaben zur Veröffentlichung / Publication details:

Campbell, Alasdair J., Michael S. Weaver, David G. Lidzey, Donal D. C. Bradley, Ekkehard Werner, Wolfgang Brütting, and Markus Schworer. 1998. "Conduction and trapping in electroluminescent polymer devices." In *Organic Light-Emitting Materials and Devices II: SPIE's International Symposium on Optical Science, Engineering, and Instrumentation, 19-24 July 1998, San Diego, CA, USA*, edited by Zakya H. Kafafi, 98–110. Bellingham, WA: SPIE.  
<https://doi.org/10.1117/12.332603>.



## Conduction and Trapping in Electroluminescent Polymer Devices

A. J. Campbell<sup>a</sup>, M. S. Weaver<sup>a,b</sup>, D. G. Lidzey<sup>a</sup>, D. D. C. Bradley<sup>a</sup>, E. Werner<sup>c</sup>,  
W. Brütting<sup>c</sup> and Markus Schwöerer<sup>c</sup>

<sup>a</sup>Centre of Molecular Materials, Department of Physics, University of Sheffield, Hicks Building, Hounsfield Road, Sheffield, S3 7RH, United Kingdom

<sup>c</sup>Lehrstuhl für Experimentalphysik II, Universität Bayreuth, 95440 Bayreuth, Germany

<sup>b</sup>Current address: Sharp Laboratories of Europe Ltd., Edmund Halley Road, Oxford Science Park, Oxford, OX4 4GA, United Kingdom

### ABSTRACT

The current-voltage (JV) characteristics of ITO/polymer film/Al or Au devices of poly(phenylene vinylene) (PPV) and a dialkoxy PPV copolymer can be fitted at high applied bias to a power law of the form  $J=KV^m$  where  $m$  increases with decreasing temperature,  $\log(K)$  is proportional to  $m$ , and  $K$  is proportional to  $d^{-\alpha m}$  where  $d$  is the film thickness and  $\alpha$  is a constant.  $\alpha \approx 2$  and  $\approx 1$  for the Al and Au cathode devices respectively. Different single carrier space charge limited conduction (SCLC) theories, involving either an exponential trap distribution or a hopping transport field and temperature dependent mobility, are used to try and explain this behaviour. Both models are in good agreement with the general experimental results, but can also be criticised on a number of specific issues. Mixed SCLC models and the effect of dispersive transport are also explored. It is concluded that carrier mobility and trap measurements are required to distinguish between these models. To this end, initial trap measurements of ITO/PPV/Al devices using deep level transient spectroscopy (DLTS) are reported. Very deep positive carrier traps with emptying times  $> 4$  minutes have been detected. The non-exponential DLTS transients have been successfully modelled on an isoelectronic trap level emptying to a Gaussian distribution of transport states, with a trap depth and density of  $\approx 0.8\text{eV}$  and  $4 \times 10^{16}\text{cm}^{-3}$  respectively.

### INTRODUCTION

Electroluminescent polymers can be used as the emissive material in organic light emitting diodes (LEDs).<sup>1,2</sup> To improve the performance of polymer LEDs it is vital to understand what mechanism(s) control the current-voltage (JV) characteristics of a given device structure. Certain device structures are injection limited, the JV characteristics being controlled by a depletion region type Schottky barrier or by thermionic or tunneling emission into an insulator. Other devices appear to be bulk limited, the characteristics being controlled by Ohmic or space charge limited conduction (SCLC). Different SCLC models have been proposed for polymer light emitting diodes (LEDs). SCLC with an exponential trap distribution has been used to model the high applied bias characteristics of poly(phenylene vinylene) (PPV) and poly(2,5-dialkoxy-*p*-phenylene-vinylene) (dialkoxy PPV) devices.<sup>3,4</sup> SCLC with a mobility found for hopping transport in disordered systems has been used to model the low applied bias characteristics of dialkoxy PPV devices and the room temperature characteristics of poly(2-methoxy,5-(2'-ethylhexoxy)-1,4-phenylene-vinylene) (MEH-PPV) devices.<sup>5-7</sup> The first part of this work will report the experimental JV characteristics of ITO/polymer film/Al or Au devices of poly(phenylene vinylene) (PPV) and a dialkoxy PPV copolymer (see Fig. 1), and the results will be discussed in terms of the different SCLC models. This analysis indicates that to distinguish between the different models it is vital to measure the presence of any traps and the field and temperature dependence of the mobility. The second part of this work deals with the measurement of traps in ITO/PPV/Al using deep level transient spectroscopy (DLTS).

### EXPERIMENTAL

The PPV precursor polymer and the dialkoxy PPV copolymer were spin coated (devices for JV characterisation) or spread with a Doctor blade (devices for DLTS) onto ITO on glass substrates (cleaned with an oxygen plasma or by refluxing in alcohol). The PPV precursor was converted under vacuum at 250°C for 6 hours (devices for JV characterisation) or 160°C for 2 hours (devices for DLTS). The PPV precursor was that with the tetrahydrothiophenium leaving group. Devices of different thicknesses ( $d$ ) of area ( $A$ ) were prepared by shadow masked Al or Au

deposition. IV characteristics were measured using a Keithley 237 source-measure unit. DLTS measurements were carried out using a Solartron Schlumberger SI1260 Impedance/Gain-Phase Analyser. Temperature measurements (accuracy  $\pm 0.1\text{K}$ ) were conducted using an Oxford Instruments CCC1204 closed cycle Helium exchange gas cryostat.

## RESULTS AND DISCUSSION

### 1. CURRENT-VOLTAGE CHARACTERISTICS

Assuming an ITO work function of approximately 4.8eV, the measured ionisation potentials and electron affinities of PPV and the dialkoxy PPV copolymer give estimated barriers to hole injection at the ITO/polymer interface of approximately 0.3 and 0.4eV respectively and electron injection at the polymer/Al interface of 1.6 and 1.1eV or at the polymer/Au interface of 2.5 and 2.0eV respectively.<sup>2,8</sup> Given in most organic materials including PPV the positive carrier mobility  $\mu_p$  is greater than the negative carrier mobility  $\mu_n$ , it can be assumed that in all of the devices the positive carrier density  $p$  is greater than the negative carrier density  $n$ .<sup>9</sup> The photoluminescent efficiencies of PPV and the dialkoxy PPV copolymer are approximately 25% and 23% respectively. However, the electroluminescent (EL) external efficiency of the ITO/polymer/Al devices are only approximately 0.002% and 0.01% respectively, whilst those of the ITO/polymer/Au devices are at least an order of magnitude lower.<sup>2,8</sup> Given that the EL efficiencies of ITO/PPV/Ca devices and state-of-the-art three layer devices are of the order of 0.1% and 1% respectively again emphasizes that in the devices in this work  $p \gg n$ .<sup>2</sup>

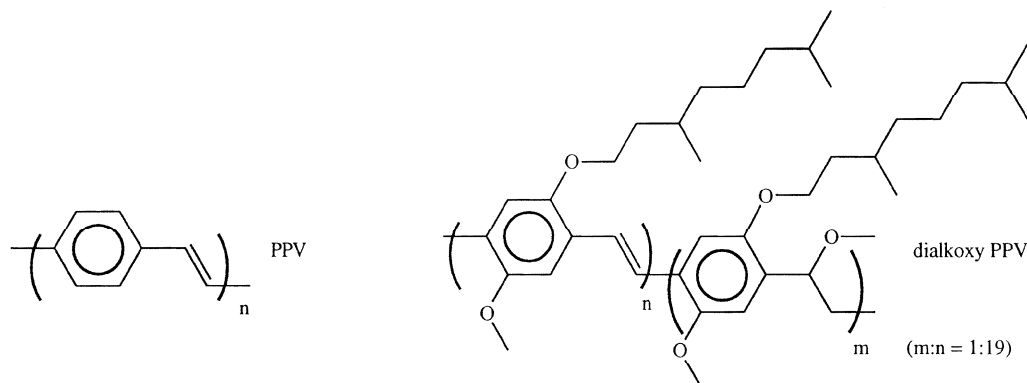


Fig. 1 Chemical structures of PPV and dialkoxy PPV.

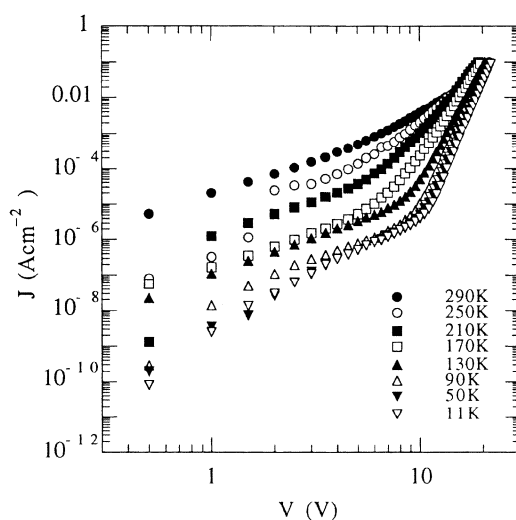


Fig. 2. Variation of the current density  $J$  with applied bias  $V$  for a 90nm thick ITO/ dialkoxy PPV copolymer/Au device.

Capacitance-voltage and impedance measurements show that both the PPV and dialkoxy PPV copolymer devices are fully depleted.<sup>3,8</sup> The JV characteristics of the devices of both polymers are also in disagreement with the predictions of Fowler-Nordheim tunneling theory for injection into an insulator.<sup>3,8</sup>

Measurements of photogeneration and transport show that the ITO/PPV contact is Ohmic.<sup>9</sup> Experimental and theoretical results also suggest that if the barrier to carrier injection at one (or both) of the injecting electrodes is less than about 0.3 to 0.4eV, conduction in single layer organic LEDs will be bulk limited.<sup>3,5</sup> It should therefore be expected that in all the device structures studied in this work the JV characteristics are dominated by the bulk limited transport of positive carriers.

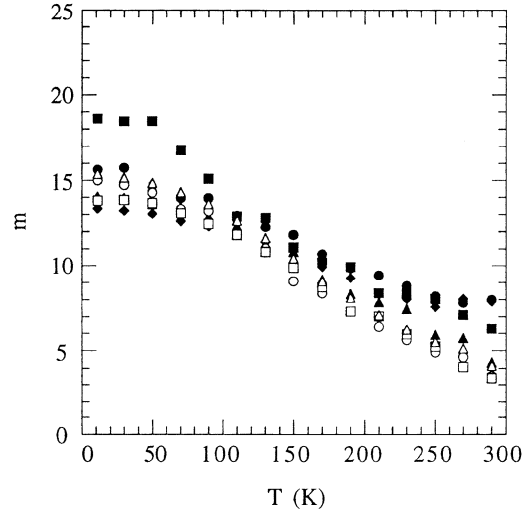


Fig. 3(a). Variation of  $m$  with  $T$  for the power law fits to the high applied bias JV characteristics of the ITO/PPV/Al devices ( $\bullet$  90nm,  $\blacksquare$  130nm), ITO/dialkoxy PPV copolymer/Al devices ( $\blacklozenge$  150nm,  $\blacktriangle$  240nm) and ITO/dialkoxy PPV copolymer/Au devices ( $\circ$  70nm,  $\square$  90nm,  $\triangle$  130nm)

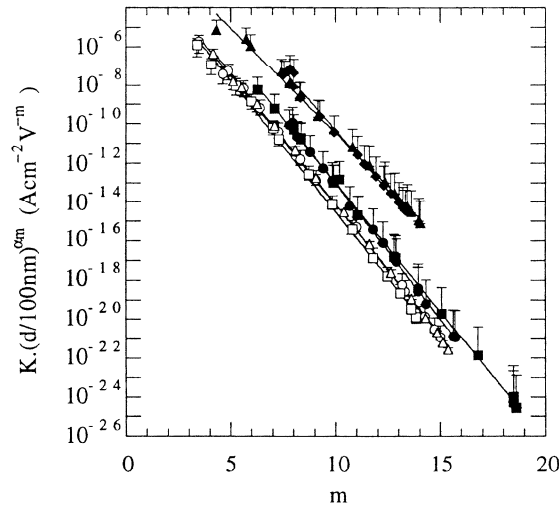


Fig. 3(b). Variation of  $K/d^{\alpha m}$  ( $d$  in units of 100nm) with  $m$  for the power law fits to the JV characteristics for all of the devices (symbols as Fig. 3(a)). The values of  $\alpha$  used are those in the text.

The JV characteristics of the ITO/PPV/Al devices and those of the ITO/dialkoxy PPV copolymer/Al and Au devices are reported in detail in ref.'s 3 and 8 respectively. Typical results for all devices measured is shown in Fig. 2. Two distinct regions can be seen in a log-log representation; a low applied bias region with a small slope, and a high applied bias region with a much larger slope. In terms of SCLC, the different regions would be explained in terms of either a change in the field dependence of the mobility and/or the movement of the Fermi level through different trap distributions in the carrier energy gap. The main difference between the

ITO/dialkoxy PPV copolymer/Al and Au devices is the thickness dependency discussed below and that the Au cathode devices require about twice the applied bias to produce the same current as the Al devices. This indicates that although the majority positive carrier current may dominate the characteristics of the Al cathode devices, a more detailed study must take into account the small negative carrier current.

The experimentally observed JV characteristics in the high applied bias regime can be analysed in terms of a power law:

$$J = KV^m \quad (1)$$

where K is a constant. This has three properties: (i) the exponent m increases with decreasing temperature T (see Fig. 3(a)); (ii) log (K) is proportional to m; (iii) the power law prefactor K is proportional to  $d^{-\alpha m}$ , where d is the polymer film thickness and  $\alpha$  is a constant (see Fig. 3(b)). The value of  $\alpha$  for each device structure was found by varying its value until the best line fits of  $\log(K/d^{-\alpha m})$  against m coincided. For the Al cathode PPV and dialkoxy PPV copolymer devices,  $\alpha = 2.1 \pm 0.3$  and  $1.9 \pm 0.3$  respectively. For the Au cathode dialkoxy PPV copolymer devices,  $\alpha = 0.8 \pm 0.1$ .

## 2. SCLC WITH AN EXPONENTIAL TRAP DISTRIBUTION

In this SCLC theory carriers are trapped by an exponential distribution of traps which lie beneath an isoelectronic distribution of transport states. As the Fermi level rises through the energy gap, trap sites below it become effectively permanently filled, no longer trapping carriers and resulting in a rapid increase of J with increasing V. The theory predicts that the JV characteristics should follow the power law Eq. (1) where the constant K is given by:

$$K = N_{\text{DOS}} \mu q \left[ \frac{\epsilon l \sin(\pi/l)}{g(\pi/l) H_t (l+1)} \right]^l \left[ \frac{(2l+1)}{(l+1)} \right]^{l+1} d^{-(2l+1)} \quad (2)$$

where  $N_{\text{DOS}}$  is the effective density of states,  $\mu$  is the mobility in the transport states, g is the trap degeneracy and  $H_t$  is the total trap density. The power law exponent m is related to the characteristic energy  $E_t$  of the exponential trap distribution by:

$$m = l + 1 = \left( \frac{E_t}{kT} \right) + 1 \quad (3)$$

so that the power law exponent m increases with decreasing temperature T. As previously shown, modelling of Eq. (2) predicts that log (K) is proportional to m.<sup>3</sup> Also, Eq.'s 2 and 3 predict that K is proportional to  $d^{-(2m-1)}$ . Given the experimentally observed values of m of between about 4 and 19,  $(2m+1) \approx 2m$ , so that K is effectively proportional to  $d^{-2m}$ . Therefore, SCLC theory with an exponential trap distribution is in very good agreement with the experimental JV characteristics, predicting a power law behaviour with the observed properties (i), (ii) and (iii).

However, this raises a number of questions. Firstly, the value of  $\alpha$  predicted by this theory is  $\approx 2$ . This is in very good agreement with the Al cathode devices, but not with the Au cathode devices. This is surprising as the theory is a single carrier model and would have been expected to be in better agreement with the Au cathode devices. Secondly, the broad optical absorption spectrum found for these materials suggests that the transport states should be distributed in energy, unlike the physical picture upon which the theory is based. Thirdly, other energetically disordered materials have a field and temperature dependent mobility, while this theory assumes a constant mobility.

Also, the experimental variation of m with T requires  $E_t$  to also vary with T, decreasing with decreasing temperature.<sup>3</sup> This can be explained in terms of the trap distribution being a steeper function of energy than that of a single exponential.<sup>3</sup> However, this could be treated as a deviation of experiment from theory.

Evidence for the existence of an exponential trap distribution in these materials comes from transient conductance measurements of PPV, the value of the distribution's characteristic energy  $E_t$  of 0.15eV agreeing very well with that found by modelling the JV characteristics of the same devices using Eq.'s (1) and (3) in this work.<sup>3</sup> Modelling of time-of-flight transient measurements of poly(1,4-phenylene-1,2-diphenoxypheyl vinylene) (DPOP-PPV) also show the presence of an exponential trap distribution with  $E_t$  of 0.04eV.<sup>10</sup>

### 3. SCLC WITH A HOPPING TRANSPORT MOBILITY

In xerographic materials the transport states are energetically disordered, carrier transport occurring by hopping between discrete molecular sites. The mobilities as measured by the time-of-flight (TOF) technique have been successfully fitted by Bässler, Borsenberger and coworkers to a temperature  $T$  and field  $F$  dependent mobility of the form:

$$\mu(T, F) = \mu_0 \exp\left(-\left(\frac{2\sigma}{3kT}\right)^2\right) \exp\left(c_0 \sqrt{F} \left(\left(\frac{\sigma}{kT}\right)^2 - \Sigma^2\right)\right) \quad (4)$$

where simulations give  $\sigma$  as the width of a Gaussian distribution of transport states and  $\Sigma$  as the level of off-diagonal disorder due to variations in inter-site coupling.<sup>11</sup> An alternative phenomenological equation sometimes used is that proposed by Gill:

$$\mu(T, F) = \mu_0 \exp\left(-\frac{\Delta_0}{kT_{\text{eff}}}\right) \exp\left(\beta \frac{\sqrt{F}}{kT_{\text{eff}}}\right) \quad (5)$$

and:

$$\frac{1}{T_{\text{eff}}} = \frac{1}{T} - \frac{1}{T^*} \quad (6)$$

where  $\Delta_0$  is the zero-field activation energy and  $T^*$  is the temperature shift factor.<sup>11</sup> Given that the conjugated polymers used in this and other works are energetically disordered, it has been suggested that the carrier transport should be very similar and that the mobilities should follow Eq.'s (4) or (5) and (6).<sup>5,6,7</sup> Here we explore this possibility for SCLC.

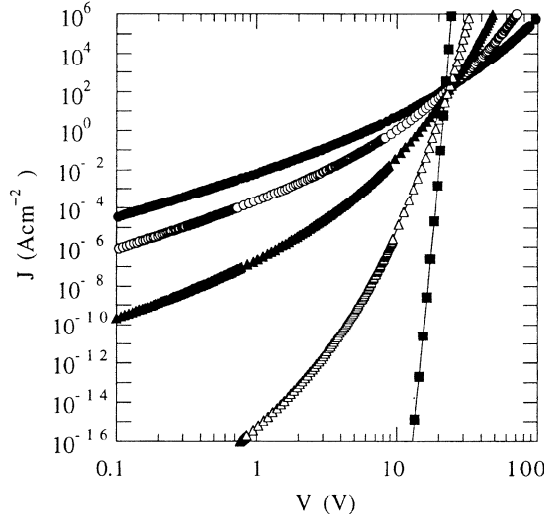


Fig. 4. Calculated JV characteristics for SCL conduction with a field and temperature dependent mobility given by the Bässler type formalism (Eq. (4)) with  $\mu_0=10^{-2} \text{ cm}^2 \text{ V}^{-1} \text{ s}^{-1}$ ,  $\sigma=0.1 \text{ eV}$ ,  $\Sigma=2$  and  $c_0=3 \times 10^{-4} \text{ cm}^{1/2} \text{ V}^{-1/2}$  and with  $\epsilon_r=3$ . This is calculated for  $d=100 \text{ nm}$  at  $kT=0.025$  (●),  $0.020$  (○),  $0.015$  (▲),  $0.010$  (△) and  $0.005 \text{ eV}$  (■) ( $T=290, 232, 174, 116$  and  $58 \text{ K}$  respectively).

The SCLC modelling involved simple numerical integration over a range of different fields  $F$ , a value of the current density  $J(F)$  for a given applied bias  $V(F)$  being calculated at the exit electrode. Typical parameters for xerographic materials and for the few values estimated for conjugated polymers were used with Eq.'s (4) or (5) and (6).<sup>6, 10-13</sup> Fig. 4 shows typical results for the Bässler type mobility. Using the Gill type mobility produced very similar JV characteristics. At high temperature and at low applied bias ( $V < 1 \text{ V}$ ) the characteristics follow a slope slightly higher than that given by Child's law of 2 expected for a field independent mobility. The slopes of the curves continuously increase with increasing applied bias and decreasing temperature. It is possible to fit all of the JV characteristics to the power law Eq. (1) over a small range of applied bias. This is shown in Fig. 5 for the Bässler type mobility. The deviation from the power law is apparent and the quality of the fit decreases with the decreasing slope of the curve. However, for comparison with experiment and as a first approximation, the curves can be fitted to Eq. (1).

Values of  $K$  and  $m$  were found by fitting the JV characteristics to Eq. (1) for applied bias between 10 and 20V. It is found for both the Bässler and Gill type mobilities that the power law exponent  $m$  increases with decreasing temperature as well as decreasing device thickness, that  $\log(K)$  is proportional to  $m$  and that  $K$  is proportional to  $d^{-\alpha m}$ .  $\alpha$  varies between 1 and 2 depending upon the parameters put into Eq.'s (4) or (5) and (6), and also increases with increasing device thickness  $d$ . Unfortunately the experimental range of  $d$  values used is not large enough to discover whether  $\alpha$  varies with  $d$ , and the scatter in Fig. 3(a) means that it is not possible to say whether the increase of  $m$  with decreasing  $d$  occurs experimentally. Therefore, SCLC theory with a hopping transport mobility, using typical parameters for the variables, is also in good agreement with the experimental JV characteristics, predicting a good approximation to a power law behaviour with the observed properties (i), (ii) and (iii).

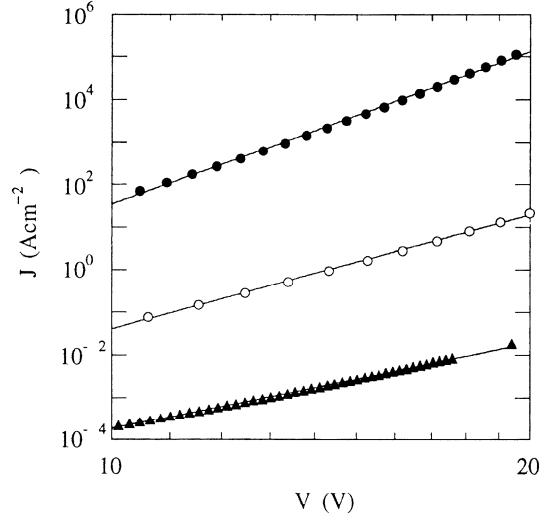


Fig. 5. The calculated JV characteristics for SCL conduction with the mobility given by the Bässler type formalism (Eq. (4)) with parameters as Fig. 4. This is calculated at  $kT=0.015\text{eV}$  ( $T=174\text{K}$ ) for  $d=50$  (●),  $100$  (○) and  $200\text{nm}$  (▲). Lines are power law fits to the characteristics from 10 to 20V of applied bias.

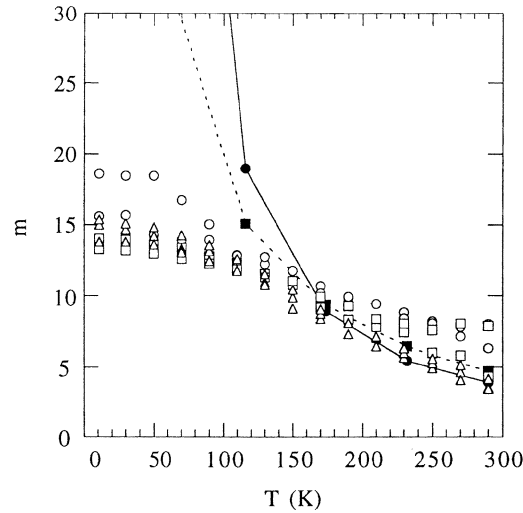


Fig. 6. Variation of the exponent  $m$  with temperature  $T$  for the power law fits of the calculated JV characteristics for SCLC with a mobility given by the Bässler (●) and Gill (■) type formalisms for  $d=100\text{nm}$  and for the power law fits of the experimental JV characteristics of the ITO/PPV/AI devices (○), ITO/dialkoxypolymer/Al devices (□) and ITO/dialkoxypolymer/Au devices (△) as shown in Fig. 3(a).

However, as for the exponential trap distribution model, there are problems with this approach. Firstly, the JV characteristics can only be fitted to a power law over about 2 orders of magnitude in  $J$ , while the experimental results in this work can be fitted for up to 4 orders of magnitude. Secondly, the values of  $K$  are between 2 and 6 orders of magnitude larger than the

values found experimentally, suggesting that if this model is correct then a large amount of trapping within the energy gap is still required. Thirdly, as is shown in Fig. 6, although the values of  $m$  calculated for both the Bässler and the Gill type mobilities appear to be in good agreement with the temperature variation of the experimental values between about 180 and 300K, below 180K the theoretical values of  $m$  increase at a much higher rate and deviate strongly from experiment. Fourthly, it is not possible to fit both the low and the high field regimes observed in the JV characteristics as this would require an abrupt and discontinuous change in the field dependence of the mobility. Although off-diagonal disorder in some xerographic materials can produce such an abrupt change, the decrease of the mobility with increasing field at low bias would not fit the results presented here.<sup>11</sup>

Unfortunately there is also relatively little experimental data from time-of-flight (TOF) measurements about the field and temperature dependence of the mobility in conjugated polymers. This is mainly due to this research area being relatively new and also the highly dispersive nature of the transients measured for most materials to date. TOF measurements of a poly(1,4-phenylene-1,2-diphenoxyphenyl vinylene) (DPOP-PPV) and transient electroluminescence measurements of PPV do show  $\log \mu \propto \sqrt{F}$ .<sup>10, 14</sup> However, TOF measurements of PPV appear to fit a  $\log \mu \propto F$  field dependence better and measurements on poly(2-phenyl-1,4-phenylenevinylene) (PPPv) appear to show a  $\log \mu \propto -\log F$  field dependence, the mobility decreasing with increasing field.<sup>12,13</sup> The variation with temperature for conjugated polymers of the TOF mobility appears to follow either an Arrhenius ( $\log \mu \propto 1/T$ ) or super-Arrhenius ( $\log \mu \propto 1/T^2$ ) relationship, which is consistent with Eq.'s (4), (5) and (6).<sup>10,12,13</sup> The TOF measurements were all recorded for fields below  $5 \times 10^5 \text{ Vcm}^{-1}$  (the transient luminescence measurement up to  $10^6 \text{ Vcm}^{-1}$ ) and for temperatures above 234K. The experimental and modelling analysis in this work using Eq. (1) was carried out for  $F(x=d) > 5 \times 10^5 \text{ Vcm}^{-1}$  and for  $T$  between 11 and 290K. Hence, although there is experimental evidence for a field and temperature dependent mobility in these materials, whether it follows Eq.'s (4), (5) and (6) still remains debatable, in particular at high fields and low temperatures.

Also, no possible explanation of the deviation of experiment from theory at low temperatures is that transport has become dispersive. Dispersion occurs because the carriers do not have time to fully relax in the transport state distribution before transiting the sample.<sup>11</sup> In this regime theoretical modelling and experiment give an apparent mobility, as measured by the transit time of the fastest carriers, of the form:

$$\mu_{\text{App.}} = \mu_0 \left( \frac{d}{F} \right)^{(1-1/\alpha_3)} \quad (7)$$

where  $\mu_0$  is a constant and  $\alpha_3$  is a parameter describing dispersive transport.<sup>11</sup> In the steady state regime the mobility would be expected to be the average value rather than that of the fastest carriers. However, if it is assumed that the steady state mobility does indeed follow Eq. (7), then for SCLC the JV characteristics should follow:

$$J = \mu_0 \epsilon \frac{(m+1)^m}{(m)^{m+1}} \frac{V^m}{d^{2m-1}} \propto \frac{V^m}{d^{2m-1}} \quad (8)$$

where  $m = 1/\alpha_3 + 1$ . This is of course exactly the relationship found experimentally between  $J$ ,  $V$  and  $d$  for large  $m$  for the Al cathode devices. One possible explanation is that because in SCLC all states at the injecting electrode are occupied, the carriers at the highest energies in the density of states distribution may never have time to completely relax crossing the device. As these are the fastest carriers, they may end up dominating the SCLC mobility with the result that the field and thickness dependence given by Eq. (7) still holds in the steady state.

#### 4. MIXED SCLC MODELS

Two different mixed SCLC models were also considered. The first considered SCLC with an exponential trap distribution but with field-assisted detrapping from that distribution. This was taken to be of a Poole-Frenkel form with a mobility given by:

$$\mu(T, F) = \mu_0 \exp\left(-\frac{\Phi_B}{kT}\right) \exp\left(\frac{\sqrt{(qF/\pi\epsilon)}}{kT}\right) \quad (9)$$



where  $\phi_B$  is the trap depth. It was assumed that the traps which dominate conduction at a given moment are those at the Fermi level  $E_F$ , so that  $E_F = \phi_B$ . The second model considered SCLC with a hopping transport mobility but also with an exponential trap distribution. Both models involved numerical integration as in Section 3. All of the JV characteristics reproduce the main features found for the SCLC with a hopping mobility model: they can be fitted over a small bias range to a power law and reproduce the experimentally observed features (i), (ii) and (iii), but with  $m$  and  $\alpha$  also varying with  $d$ .

However, in both models the slope  $m$  increases more rapidly with temperature than that found in the hopping mobility models, thus exasperating the deviation from experiment. Secondly, both models may be criticised as being physically unreasonable in assuming that all of the transport states lie at a single energy.

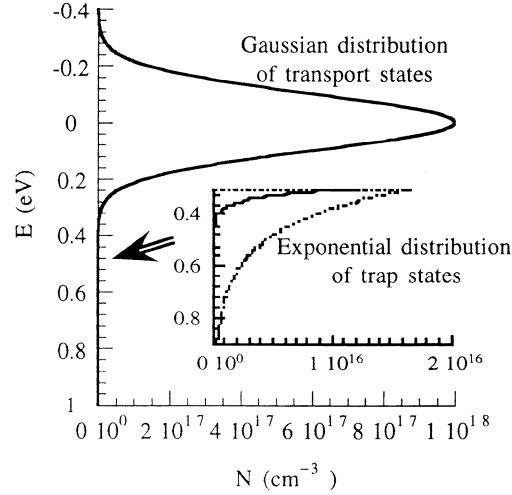


Fig. 7(a). Gaussian distribution of transport states with  $\sigma=0.1\text{eV}$  and a total density of  $10^{20}\text{cm}^{-3}$  with an exponential distribution of trap states at  $0.3\text{eV}$  with  $E_t=0.15\text{eV}$  and a total density of  $10^{18}\text{cm}^{-3}$ .

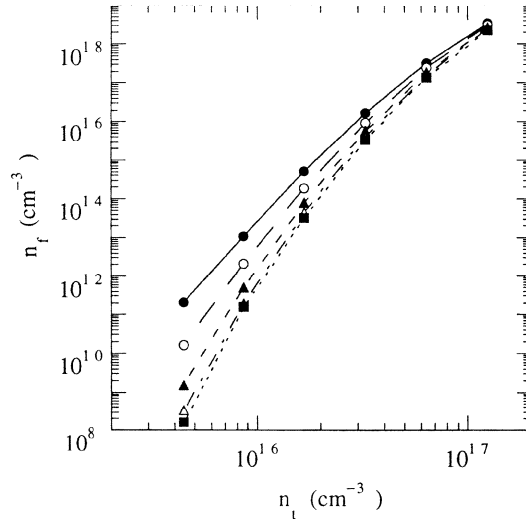


Fig. 7(b) Variation of the free carrier density  $n_f$  in the transport states with the trapped carrier density  $n_t$  in the trap states in Fig. 7(a) as the quasi Fermi level rises in the energy gap. This is calculated at  $kT=0.025$  ( $\bullet$ ),  $0.020$  ( $\circ$ ),  $0.015$  ( $\blacktriangle$ ),  $0.010$  ( $\triangle$ ) and  $0.005\text{eV}$  ( $\blacksquare$ ) ( $T=290, 232, 174, 116$  and  $58\text{K}$  respectively).

## 5. SCLC WITH A BROAD TRANSPORT STATE DISTRIBUTION

One of the criticisms of the SCLC models which involve an exponential trap distribution is that they all assume that the transport states are isoelectronic. This results in a relationship

between the free carriers  $n_f$  in the isoelectronic transport states and the trapped carriers  $n_t$  in the exponential trap distribution (free carriers carry the current, trapped carriers do not) of the form:

$$n_f = \Theta n_t^l \quad (10)$$

where  $l$  is given by Eq. (3) and:

$$\Theta = N_{\text{DOS}} \left( \frac{(\pi/l)}{gH_t \sin(\pi/l)} \right)^l \quad (11)$$

It is from this power law relationship that all of these models are derived. However, if the isoelectronic transport states are replaced by a Gaussian distribution as shown in Fig. 7(a), then the resultant relationship between  $n_f$  and  $n_t$  is shown in Fig. 7(b). Over about 4 or 5 decades of  $n_f$ , Eq. (10) does indeed appear to be a good approximation to the relationship between the free and trapped carriers. Hence, the SCLC models which involve an exponential trap distribution appear to work equally well with a more realistic Gaussian distribution of transport states.

The results in Fig. 7(b) also show that the slope of the curves vary with carrier density, so that any deviations of the experimental JV characteristics from the power law Eq. (1) can be explained in terms of some type of transport state distribution.

## 6. DEEP LEVEL TRANSIENT SPECTROSCOPY

It is apparent that all of the SCLC models are in general agreement with the experimental observations and that it is very difficult to distinguish between them. The only way to reliably do this is to independently measure the carrier mobilities and the presence of any traps, and then use the resultant quantities in the SCLC models. Any information about these quantities is therefore vital for any attempt at modelling transport in these materials.

One technique used to study traps in inorganic semiconductors is deep level transient spectroscopy (DLTS). Traditional DLTS requires the presence of a depletion region. However, nearly all polymer LED devices are fully depleted.<sup>3,8</sup> One notable exception are the thick ( $\approx 500\text{nm}$ ) ITO/poly(phenylene vinylene) (PPV)/metal devices constructed by the group at Universität Bayreuth. These contain enough extrinsic "accidental" dopants to form a depletion region type Schottky barrier at the polymer/metal interface.<sup>15</sup>  $\text{InCl}_3$  compounds are produced during the thermal conversion of the PPV precursor on the ITO substrate.<sup>17</sup> These act as p-type acceptor dopants with a typical density  $N_a$  of between  $10^{16}$  and  $10^{17} \text{ cm}^{-3}$ . Typical ITO/PPV/Al devices have a diffusion potential  $V_d$  of between 1.1 to 1.5eV and a depletion region width  $w_d$  of between 50 and 150 nm.<sup>15,17</sup>

In the DLTS technique, the device is held under a quiescent bias  $V_{QB}$  at which it will have a depletion region width  $w_d$ . A positive voltage pulse  $V$  is then applied, decreasing the depletion region width. Any traps which intersect the Fermi level in the depletion region will be pulled beneath it and filled. When the positive bias is removed, the depletion region will expand back towards  $w_d$  and the trap levels which have been filled will rise above the Fermi level. These will then empty at a rate depending upon their depth beneath the transport states. The depletion region width depends upon the amount of charge stored within the depletion region. Hence, as the traps empty, the width will slowly return to the value it had under  $V_{QB}$  before the voltage pulse was applied. The width is directly related to the measured capacitance  $C$ . Hence, the variation of the capacitance with time can be used to measure the decay of trapped charge within the depletion region.

For emptying of a single majority carrier trap level (for  $N_a \gg N_t$ ):

$$C(t) = C(w_d) \left( 1 - \frac{1}{2(N_a - N_t)} \left\{ \frac{x_1^2 - x_2^2}{w_d^2} \right\} n(t) \right) \quad (12)$$

$$n(t) = N_t \exp(-e_p t) \quad (13)$$

$$e_p = \frac{\sigma_{\text{cap}} N_{\text{DOS}} \langle v \rangle}{g} \exp\left(-\frac{E_t}{kT}\right) \quad (14)$$

where  $N_a$  is the acceptor dopant density,  $N_t$  is the trap density,  $x_1$  and  $x_2$  are the two positions in the depletion region between which the traps are filled,  $e_p$  is the trap emission rate,  $E_t$  is the trap energy,

$\sigma_{\text{cap}}$  is the trap capture cross section,  $N_{\text{DOS}}$  is the density of transport states,  $\langle v \rangle$  is the carrier thermal velocity and  $g$  is the trap degeneracy.

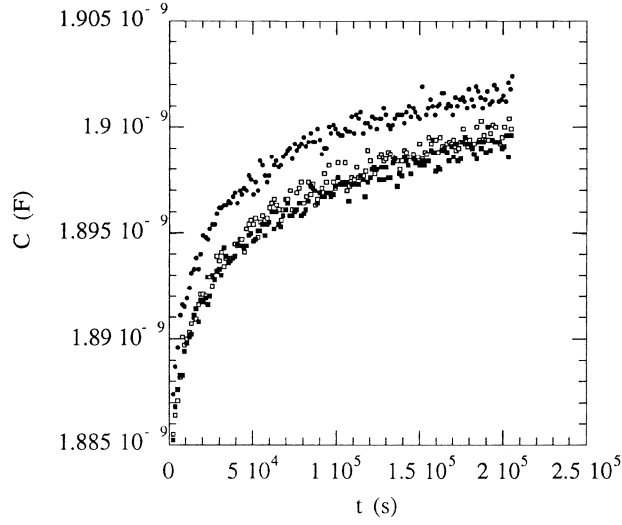


Fig. 9(a) DLTS transient for a 200nm thick ITO/PPV/Al device. Recorded at 282K,  $V_{\text{QB}} = -1\text{V}$ ,  $V = +1\text{V}$ , pulse length = 10s, measurement frequency = 97Hz and sampling rate = 1s.

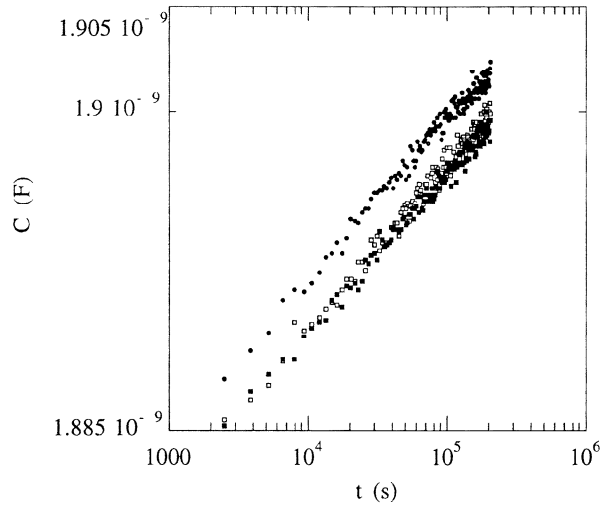


Fig. 9(b) As 9(a) but on a log-log representation.

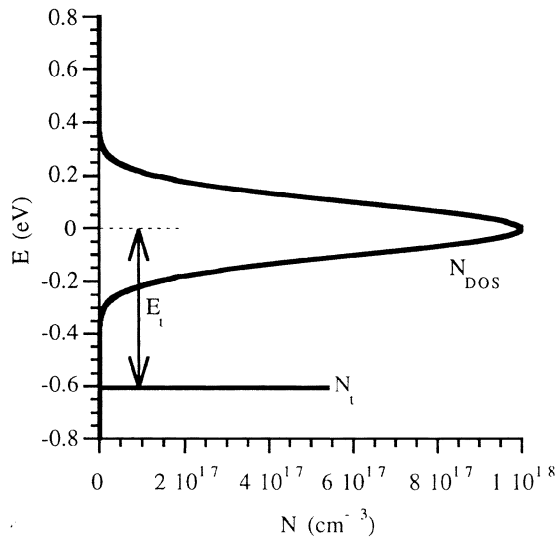


Fig. 10. An isoelectronic trap level lying below a Gaussian distribution of transport states.

Typical results are shown in Fig. 9. Capacitance-voltage measurements gave  $N_a$  of  $3 \times 10^{17} \text{ cm}^{-3}$  and  $V_d$  of about 2V for these devices. The DLTS transients last for over 4 minutes, indicating that the traps are very deep in the energy gap. The capacitance increases with time, indicating that these are majority carrier p-type traps. On a log-log representation it is clear that the transients are non-exponential. Therefore, the transients cannot be modelled on a single energy trap level emptying to isoelectronic transport states. Instead, either the traps or the transport states must be distributed in energy.

These results have been modelled on the physical situation shown in Fig. 10 of an isoelectronic trap level emptying to a Gaussian distribution of transport states. The charge  $n(t)$  in the trap states time  $t$  is calculated by integrating over a Gaussian distribution of emission rates:

$$n(t) = \int N_{\text{Gaus.}}(E_t) \exp(-e_p(E_t)t) dE_t \quad (15)$$

The capacitance  $C(t)$  at time  $t$  is then calculated using Eq. (12). The model assumes that there is no retrapping and that the attempt-to-escape frequency  $\frac{\sigma_{\text{cap}} N_{\text{DOS}} \langle v \rangle}{g}$  is constant.

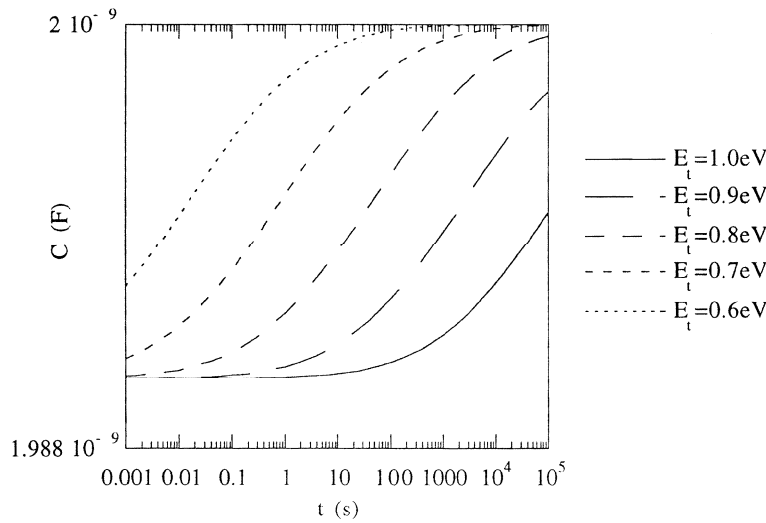


Fig. 11. Calculated capacitance transients for the emptying of an isoelectronic trap level to a Gaussian distribution of transport states. For a Gaussian width  $\sigma = 0.1 \text{ eV}$ ,  $kT = 0.025 \text{ eV}$ ,

$$\frac{1}{2(N_a - N_t)} \left\{ \frac{x_1^2 - x_2^2}{w_d^2} \right\} = 0.005, \text{ attempt-to-escape frequency} = 10^{12} \text{ s}^{-1} \text{ and } C(w_d) = 2 \text{ nF.}$$

The resultant capacitance transients are shown in Fig. 11 on a log-log representation. It is found that the slope of the linear region on this log-log representation increases with increasing temperature  $T$ , increasing trap density  $N_t$  and decreasing Gaussian width  $\sigma$ . Assuming that  $\sigma$  lies between 0.06 and 0.12 eV and the attempt-to-escape frequency lies between  $10^{10}$  and  $10^{14} \text{ s}^{-1}$ , modelling the experimental  $C(t)$  transients shown in Fig. 9(b) on the linear region of the log-log representation gives  $E_t = 0.8 \pm 0.1 \text{ eV}$  and  $N_t = 4 \pm 1 \times 10^{16} \text{ cm}^{-3}$ . The value of  $E_t$  is in very good agreement with thermally stimulated current measurements of traps associated with the presence of oxygen in similar devices. Conductivity and positive carrier time-of-flight measurements in similar devices also have the same activation energy.

## 7. CONCLUSIONS

Different single carrier space charge limited conduction (SCLC) theories, involving either an exponential trap distribution or a hopping transport field and temperature dependent mobility or a combination of both, have been used to try and explain the current-voltage characteristics of ITO/polymer film/Al or Au devices of poly(phenylene vinylene) (PPV) and a dialkoxy PPV copolymer. All of the models are in good agreement with the general experimental

results, but all can be criticised on a number of specific issues. The models are also very difficult to distinguish between each other. The only way to resolve the nature of SCLC in these materials is by experimental measurements of the field and temperature dependence of the mobility and the depth and density of any traps in the energy gap. Deep level transient spectroscopy (DLTS) measurements have identified at least one positive carrier trap in PPV devices, and this must be taken into account in any future modelling.

## 8. ACKNOWLEDGEMENTS

The authors would like to thank Karl Pichler of Cambridge Display Technology Ltd., Cambridge, U.K. for supplying the PPV precursor polymer for the JV characterisation devices and Emiel Staring of Philips Research Laboratories, Eindhoven, The Netherlands for supplying the dialkoxy PPV copolymer. The Authors would also like to thank the E.P.S.R.C., U.K. for funding through grant GR/K57428.

## 9. REFERENCES

1. D. D. C. Bradley, "Electroluminescent polymers: materials, physics and device engineering", *Current Opinion in Solid State & Mat. Sci.* **1**, pp. 789-797, 1996
2. D. D. C. Bradley, "Conjugated polymer electroluminescence" *Synth. Met.* **54**, pp. 401-415, 1993
3. A. J. Campbell, D. D. C. Bradley and D. G. Lidzey, "Space Charge Limited Conduction in poly(phenylene vinylene) Light Emitting Diodes", *J. Appl. Phys.* **82**, p. 6326, 1997
4. P. W. M. Blom, M. J. M. de Jong and J. J. M. Vleggaar, "Electron and hole transport in poly(*p*-phenylene vinylene) devices", *Appl. Phys. Lett.* **68**, pp. 3308-3310, 1996
5. P. S. Davids, I. H. Campbell and D. L. Smith, "Device Model for Single Carrier Organic Diodes", *J. Appl. Phys.* **82**, p. 6319, 1997
6. P. W. M. Blom, M. J. M. de Jong and M. G. van Munster, "Electric-field and temperature dependence of the hole mobility in poly(*p*-phenylene vinylene)", *Phys. Rev. B* **55**, pp. R656-R659, 1997
7. E. M. Conwell and M. W. Wu, "Contact injection into polymer light-emitting diodes" *Appl. Phys. Lett.* **70**, pp. 1867-1869, 1997
8. M. S. Weaver, PhD Thesis, University of Sheffield, U.K. (1997)
9. H. Antoniadis, J. N. Miller, d.B. Roitman and I. H. Campbell, "Effects of Charge Carrier Injection in Organic Light Emitting Diodes" *IEEE Trans. on Electron Devices* **44**, pp. 1289-1294, 1997
10. H. Meyer, D. Haarer, H. Naarmann and H. H. Horhold, "Trap distribution for charge carriers in poly(phenylene vinylene) (PPV) and its substituted derivative DPOP-PPV", *Phys. Rev. B* **52**, pp. 2587-2598, 1995
11. H. Bassler, "Charge transport in disordered organic photoconductors", *Phys. Stat. Sol. (b)* **175**, pp. 15-56, 1993
12. M. Gailberger and H. Bassler, "DC and transient photoconductivity of poly(2-phenyl-1,4-phenylenevinylene)" *Phys. Rev. B* **44**, pp. 8643-8651, 1991
13. E. Lebedev, Th. Dittrich, V. Petrova-Koch, S. Karg and W. Brütting, "Charge carrier mobility in poly(*p*-phenylene vinylene) studied by the time-of-flight technique", *Appl. Phys. Lett.* **71**, pp. 2686-2688, 1997
14. S. Karg, V. Dyakonov, M. Meier, W. Reiss and G. Paasch, "Transient electroluminescence in poly(*p*-phenylene vinylene) light-emitting diodes", *Synth. Met.* **67**, pp. 165-168, 1994
15. M. Meier, S. Karg and W. Riess, "Light-emitting diodes based on poly-*p*-phenylene-vinylene: II. Impedance spectroscopy", *J. Appl. Phys.* **82** pp. 1961-1966, 1997
16. M. Meier, S. Karg, K. Zuleeg, W. Brütting and M. Schwoerer, "Determination of trapping parameters in PPV light-emitting-devices using thermally stimulated currents", submitted to *J. Appl. Phys.*
17. W. Brütting, M. Meier, M. Herold and M. Schwoerer, "Control of impurities in PPV light emitting devices", *Synth. Met.*, **91** pp.163-168, 1997
18. S. Karg, W. Reiss, V. Dykonov and M. Schwoerer, "Electrical and optical characterization of poly(*p*-phenylene vinylene) light emitting diodes" *Synth. Met.*, **54** pp. 427-433, 1993